

# Study on Optimum Geometric Dimensions of Micro-Forming Taps (MFTs) in SUS 316L Stainless Steel Tapping

Hsing-Ming Teng\*, Chien-Chung Chen\*\*, Yung-Han Hsu\*\*\*,  
Ming-Chang Wu\*\*\*\*, Ling-Sheng Hsu\*\*\*\*\*  
and Chung-Chen Tsao\*\*\*\*\*

**Keywords :** micro-forming tap, Box-Behnken design, tooth filling rate, regression analysis, minimum tapping torque.

well as the optimum geometric parameters of MFT obtained in this study are quite accurate and consistent.

## ABSTRACT

This study aims to develop a new tapping tool design based on the geometric parameters (outer diameter ( $D$ ), tool width ( $W$ ), tooth root diameter ( $D_2$ ) and length of the invalid tooth ( $L$ )) of the MFT to overcome the problem of using traditional tap on the defects of tool breakage (tapping torque), low processing efficiency and chip removal during SUS 316L stainless steel tapping. Simultaneously, the second-order response surface model of quality characteristics was established through Box-Behnken design (BBD) and regression analysis, and the optimal tool geometric parameters for the minimum tapping torque ( $T$ ) and tooth filling rate ( $f$ ) of M1.2 tungsten carbide MFTs in SUS316L stainless steel tapping was discussed. Finally, the experimental results show that the  $T$  and  $f$  prediction models, as

*Paper Received July, 2023. Revised September, 2023. Accepted November, 2023. Author for Correspondence: Chung-Chen Tsao.*

\* Graduate student, Department of Industrial Education, National Taiwan Normal University, Taipei 106308, Taiwan, ROC

\*\* Assistant Professor, Department of Intelligent Vehicles and Energy, Minsh University of Science and Technology, Hsinchu 307304, Taiwan, ROC

\*\*\* Graduate student, Department of Mechanical Engineering, National Central University, Taoyuan, 32054, Taiwan, R.O.C.

\*\*\*\* Associate Professor, Department of Mechanical Engineering, Lunghwa University of Science and Technology, Taoyuan, Taiwan 333326, ROC.

\*\*\*\*\* Boss, He Zuan Machine Co., Ltd., Hsinchu 307001, Taiwan, ROC

\*\*\*\*\* Professor, Department of Mechanical Engineering, Lunghwa University of Science and Technology, Taoyuan, Taiwan 333326, ROC.

## INTRODUCTION

As the times change, consumers' demand for thinner, smaller, and multi-functional 3C smart electronic products is increasing. The materials commonly used in 3C smart electronic products are aluminum alloy, stainless steel and titanium alloy. Among them, in terms of price, mechanical properties and machinability, stainless steel is just between aluminum alloy and titanium alloy. Because the corrosion resistance and strength of SUS 316L stainless steel are far superior to that of aluminum alloy, and it is widely used in internal structural parts such as antennas, batteries, and charging sockets in smartphones. The requirements for the number and accuracy of locking internal threads used in 3C smart electronic products have also increased, and the size of internal threads has also dropped significantly to below 2 mm. For example, there are 77 internal threads inside an iPhone 8 plus mobile phone. In order to cope with this huge capacity of internal threads, the geometric shape and processing efficiency of the tapping must be carefully considered. However, the internal thread is the last processing procedure that needs to be produced by tapping the finished product. The quality of the internal thread will directly affect the smoothness and integration of the product. Among the small internal thread processes, the direct relation of the micro-tapping tool on the geometric dimensions and quality characteristics ( $T$  and  $f$ ) is of a special interest. The micro-tapping tool induces a forming and extrusion actions in the metal material, which has many interesting effects on the  $T$  and the  $f$ . Therefore, optimizing the geometry parameters of the micro-tapping tool to improve the quality of the small

internal thread is the focus of many scholars' study.

MFT is currently the most versatile used tool for making internal threads (blind hole) of 3C smart electronic products, and its size is mostly M1.2×0.25 mm. The micro-forming tapping process mechanism aims to use its own geometry to force the plastically deformed material to adhere to the shape of the MFT to flow to form internal threads. Therefore, the geometric shape of the MFT is related to the  $T$  and  $f$  are inextricably linked. Since the MFT does not produce any chips in tapping, it does not need to have a flute design, so it has a larger tooth root diameter and rigidity than the traditional tap of the same specification, and 2 to 3 times the tapping torque. During actual processing, MFTs can be tapped at a higher speed to improve processing efficiency and reduce manufacturing costs. Agapiou found that when the tapping speed of forming tap increases, the  $T$  will decrease slightly, and the  $f$  will increase. The difference in geometry of forming taps will significantly affect the filling rate of the tooth profile and the maximum tapping torque, but has little effect on the thrust force. Ivanov summarized a number of mathematical equations based on the process parameters and geometric design of the forming tap, and effectively improved the life of the forming tap and improved the internal thread processing efficiency, and proved that non-ferrous metals are very suitable perform forming tapping. Chowdhary et al. used the rigid-plastic model to predict the torque of the forming tap when forming the internal thread. When the forming speed is 250~1,000 rpm, the predicted tapping torque is always lower than the experimental value. Simultaneously, the simulation results show that the lead angle length of the forming tap has no effect on the axial force, but a smaller lead angle length will increase the tapping torque and accelerate the wear of the cutting edge of the forming tap. Mathurin et al. used finite element software to confirm that the aperture under the forming tap is the biggest factor affecting the tapping torque, while the forming speed has a less significant effect on the tapping torque. Stéphan et al. used the slip-line method, and considered the geometry and elastic recovery of the tool itself, to obtain a model that generates the maximum tapping torque when forming the side of the internal thread. The analysis results show that the diameter of the hole under the forming tap and the length of the invalid tooth ( $L$ ) have the greatest influence on the tapping torque. Hou et al. found the optimal processing conditions (tooth root diameter, forming speed and friction factor) can reduce the maximum tapping torque by 37.15%, and the degree of forming and plastic deformation of the top, side, and root of the thread profile are different. In practice, the  $f$  must reach 75% to meet the ISO standard (ISO 68-1). Warrington et al. found that the size of the split crest is related to the filling rate of the tooth form. When the filling rate of the tooth form

increases, the metal material on both sides of the split crest is saturated, and finally a void is formed at the top of the thread.

In some early studies (Agapiou, 1994; Sakurai et al., 2006; Carvalho et al., 2012; Tállai et al., 2015; Landeta et al., 2015) the size of the forming taps discussed is too large, and the material is high-speed steel, and the geometry of the tungsten MFTs is rarely discussed. The impact of geometry shape and process parameters on the  $f$  and  $T$  (two quality characteristics), so this study uses the tool geometric parameters ( $D$ ,  $W$ ,  $D_2$  and  $L$ ), combing BBD to establish a two-quality characteristic response surface model, to discuss the optimal tool geometry of the  $f$  and  $T$  of M1.2 tungsten carbide MFTs in SUS 316L stainless steel tapping combination of parameters. The geometric dimension of the MFT as shown in Fig. 1.

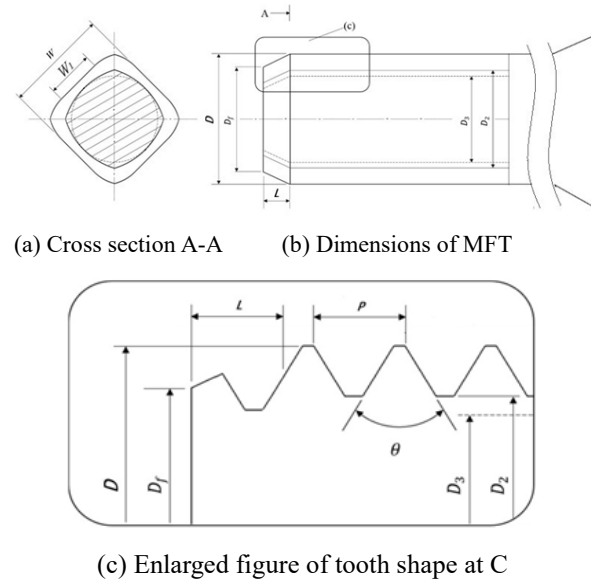


Fig. 1. The geometric dimension of the MFT

## DESIGN OF EXPERIMENTS

### Response surface method (RSM) and BBD

RSM is a set of statistical and mathematical techniques effectively used to develop, improve, analyze and optimize manufacturing processes. It can interpret the individual and interactive problems of multiple independent variables  $x_i$  (quality parameters) through experimental design and regression analysis, and obtain the most beneficial response function  $y_i$  (quality characteristics) information with the least experimental time and cost to assist the user performs quality parameter optimization. In addition, regression analysis is a numerical method based on mathematical induction by which patterns of empirical or quality characteristics can be constructed. It can analyze the functional relationship between one or more independent variables and dependent

variables, establish a regression model, estimate regression coefficients, and find an appropriate approximation function with the least square method. Since the second-order model can present the reaction function more accurately and has a better ability to explain the construction model, this study uses the second-order model to construct the minimum tapping torque ( $T$ ) and tooth filling rate ( $f$ ) of the micro-forming tapping. The general formula of the second-order model function can be expressed as follows:

$$y = \beta_0 + \sum_{i=1}^k \beta_i x_i + \sum_{i=1}^k \sum_{j=1}^k \beta_{ij} x_i x_j + \sum_{i=1}^k \beta_{ii} x_i^2 + \varepsilon \quad (1)$$

where,  $y$  is the quality characteristic,  $x_i$  is the  $i^{\text{th}}$  experimental parameter,  $\beta_0$  is the coefficient of the constant term,  $\beta_i$  is the coefficient of the  $i^{\text{th}}$  experimental parameter,  $\beta_{ij}$  is the coefficient of the interaction term between the  $i^{\text{th}}$  and  $j^{\text{th}}$  experimental parameters and  $\beta_{ii}$  is the second-order term of the experimental parameter and  $\varepsilon$  is the model error.

BBD is an important second-order RSM, which can observe the influence of experimental points with different quality parameters from central point experiments on  $T$  and  $f$ . Therefore, this paper uses the BBD to plan a tapping experiment table with four quality parameters and three levels, as shown in Table 1. Nos. 25-28 are four groups of center point repeat experiment points.

Table 1. Table of BBD

No.	$D$	$W$	$D_2$	$L$
1	-1	-1	0	0
2	-1	1	0	0
3	1	-1	0	0
4	1	1	0	0
5	-1	0	-1	0
6	-1	0	1	0
7	1	0	-1	0
8	1	0	1	0
9	-1	0	0	-1
10	-1	0	0	1
11	1	0	0	-1
12	1	0	0	1
13	0	-1	-1	0
14	0	-1	1	0
15	0	1	-1	0
16	0	1	1	0
17	0	-1	0	-1
18	0	-1	0	1
19	0	1	0	-1
20	0	1	0	1
21	0	0	-1	-1
22	0	0	-1	1
23	0	0	1	-1
24	0	0	1	1
25	0	0	0	0
26	0	0	0	0
27	0	0	0	0
28	0	0	0	0

**Experimental factors and levels**

The geometrical and dimensional characteristics of MFTs are critical to the tapping quality. This study mainly discusses the influence of geometric parameters of MFT on SUS 316L stainless steel tapping, taking  $f$  and  $T$  as quality characteristics, and selecting  $D$ ,  $W$ ,  $D_2$  and  $L$  as quality parameters. The optimal design of MFT for SUS 316L stainless steel tapping is aimed at increasing  $f$  to 85% (target) and reducing  $T$  (minimum).  $f$  is selected as 85%, which can avoid the tooth shape not conforming to the ISO specification caused by too low  $f$ , or avoid the assembly interference problem caused by too high  $f$  (Oliveira et al., 2019). As for the smaller  $T$ , the risk of sudden breakage of the MFT during tapping can be reduced, and the wear of the tool can be reduced. In addition, when selecting the level of quality parameters in this study, the geometric dimensions of tools commonly used in the 3C industry are used as the optimal center point, and the upper and lower limits of each quality parameter level are defined based on the optimal center point, and the level value represented by coding variables -1, 0, and 1, as shown in Table 2.

Table 2. Selected quality parameters and levels

Level	$D$ (mm)	$W$ (mm)	$D_2$ (mm)	$L$ (mm)
1	1.255	1.05	0.975	0.75
0	1.245	1.00	0.950	0.50
-1	1.235	0.95	0.925	0.25

**EXPERIMENTAL PROCEDURE**

In order to understand the quality characteristics of MFTs in SUS 316L stainless steel tapping, this study experiment was carried out on Brother S500X1 machining center, and the SUS 316L workpiece was fixed on the self-made fixture. The size of the SUS 316L workpiece used for tapping is 40mm×40mm×5mm. As for the process parameters of the micro-forming tapping experiment, as shown in Table 3. When measuring the tapping torque of the MFT on SUS 316L stainless steel, the KISTLER 9273 dynamometer outputs the weak voltage signal received on the tapping workpiece, and through the KISTLER 5011B signal amplifier and NI-6110S data acquisition card, the extracted tapping torque values are sent to the LabVIEW man-machine system for experimental monitoring. After the tapping is completed, the data is stored in the personal computer for subsequent data sorting and analysis. In order to reduce the measurement error of the tapping torque experiment, the micro-forming tapping at the same experimental point will be repeated 9 times in this study. As shown in Fig. 2, the MFT in SUS 316L stainless steel is set up for the tapping experiment.



Fig. 2. Photograph of the experimental setup by micro-forming tapping

Fig. 3 is a graph showing the relationship between the tapping torque and time of the MFT. Mark(a) is that the front end of the MFT starts to contact the SUS 316L workpiece, so the tapping torque is zero. As the MFT gradually enters the SUS 316L workpiece, the tapping torque begins to increase, and the tapping depth of the MFT is about 0.191 mm (mark (b)). Guided by the length of the invalid tooth ( $L$ ), the MFT is gradually introduced into the pre-drilled guide hole. At this time, the  $L$  begin to extrude the metal material, and the contact surface between the MFT and the SUS 316L workpiece continues to increase, and the tapping torque starts to increase rapidly, and the tapping depth of the MFT is about 0.75mm (mark (c)). However, as the depth of the MFT into the SUS 316L workpiece increases, the metal material formed by the MFT gradually decreases, and the change in the tapping torque gradually slows down. The tapping torque of the MFT reaches the maximum value, and the tapping depth reaches 1.5mm (mark (d)), the machine stops tapping and remains in a static state, and there is no tapping torque at this time. Then the MFT starts to retract in the reverse direction. Affected by the friction force between the SUS 316L workpiece and the MFT, the tapping torque is the largest at this time. As the MFT gradually withdraws from the SUS 316L workpiece, the friction force between the SUS 316L workpiece and the MFT decreases, and the tapping torque gradually decreases (mark (e)), until the MFT completely exits the SUS 316L workpiece, and the tapping torque is zero (mark (f)), and the entire formed thread tapping experiment of MFT is completed.

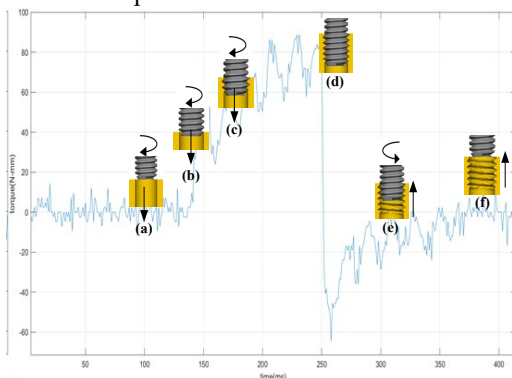


Fig. 3. Relationship between the tapping torque and time of the MFT

The SUS 316L workpiece after the tapping experiment was then preprocessed for tooth profile measurement with a wire cutting machine (CHMER 4025L) and a grinding and polishing machine (TNP-2020FR). An optical microscope (OLYMPUS STM7-MF) and digital camera (OLYMPUS DP27) were used to take pictures of the tooth profile of the SUS 316L workpiece after micro-forming tapping, and then use the ImageJ image analysis software to binarize the tooth profile, and use the particle analysis function to calculate the tooth profile area. In order to reduce the measurement error of the tooth-shaped area experiment, the tooth-shaped area of all SUS 316L workpieces was measured three times. The calculation of  $f$  in this study is shown in Eq. 2.

$$f = A_T / A_I \times 100\% \quad (2)$$

where  $A_T$  is the tooth profile area of the SUS 316L workpiece,  $A_I$  is the ideal tooth profile area, and its value is  $0.01974 \text{ mm}^2$ .

Table 3. Tapping process parameters

Terms	Value
Workpiece material	SUS 316L stainless steel
Lubricating oil	Castrol Alusol SL51 XBB (water soluble 15%)
Plate thickness (mm)	5.0
Pre-drill hole depth (mm)	2.0
Smaller hole diameter (mm)	1.10
Processing stroke (mm)	1.5
Feed rate (mm)	125
Spindle speed (rpm)	500
Tool specifications	<b>M1.2 × 0.25 mm</b>
Tool material	Tungsten carbide

## RESULTS AND DISCUSSION

### Factor analysis

The experimental results on  $f$  and  $T$  for MFTs are shown in Table 4. To understand the relationship between the quality parameters and the quality characteristics for MFTs for tapping in SUS 316L stainless steel, a second-order regression model was determined using MINITAB software, which generates the prediction equations for the thread filling rate ( $f_1$ ) and the minimum tapping torque ( $T_1$ ). These second-order regression models for  $f_1$  and  $T_1$  are expressed as follows:

$$f_1 = 85.80 + 2.494D + 0.888W - 0.968D_2 - 3.872L + 0.549D^2 - 2.65W^2 - 3.682D_2^2 - 0.618L^2 - 0.168DW - 0.76DD_2 + 0.35DL + 0.228WD_2 + 3.26WL + 0.827D_2L \quad (3)$$

$$T_1 = 61.435 + 9.978D + 7.927W + 3.072D_2 - 0.313L + 5.618D^2 + 4.785W^2 + 3.075D_2^2 + 3.223L^2 - 3.15DW + 2.665DD_2 - 1.553DL - 0.768WD_2 - 3.745WL - 2.065D_2L \quad (4)$$

where  $D$  is the outer diameter,  $W$  is the tool width,  $D_2$  is the tooth root diameter and  $L$  is the length of invalid teeth. From Eqs. (3) and (4),  $D$  and  $W$  have a positive correlation on  $T_1$  and  $f_1$ , while  $L$  has a negative correlation on  $T_1$  and  $f_1$ . As for the relationship that  $D_2$  has a positive correlation at  $f_1$  and a negative correlation at  $T_1$ . When  $D$  and  $W$  increase or  $L$  decreases, it is easier for the metal material to be processed to generate flow, thus increasing  $T_1$  and  $f_1$ . When  $D_2$  increases,  $T_1$  increases, and  $f_1$  decreases, because it is necessary to push the processing materials around the tooth crest and root to generate metal flow (Mathurin et al., 2009).

Table 4. Experimental results of BBD

No.	$D$	$W$	$D_2$	$L$	$f_1$ (%)	$T$ (N-mm)
1	-1	-1	0	0	80.06	50.75
2	-1	1	0	0	82.04	72.74
3	1	-1	0	0	85.77	77.53
4	1	1	0	0	87.08	86.92
5	-1	0	-1	0	80.36	60.35
6	-1	0	1	0	79.66	61.68
7	1	0	-1	0	87.08	72.74
8	1	0	1	0	83.34	84.73
9	-1	0	0	-1	87.72	58.35
10	-1	0	0	1	79.39	60.75
11	1	0	0	-1	91.41	83.12
12	1	0	0	1	84.48	79.31
13	0	-1	-1	0	79.31	58.15
14	0	-1	1	0	77.50	63.67
15	0	1	-1	0	81.02	73.60
16	0	1	1	0	80.12	82.19
17	0	-1	0	-1	88.57	58.15
18	0	-1	0	1	74.86	65.34
19	0	1	0	-1	83.57	80.53
20	0	1	0	1	82.90	72.74
21	0	0	-1	-1	87.69	63.89
22	0	0	-1	1	77.62	67.15
23	0	0	1	-1	83.80	72.74
24	0	0	1	1	77.04	67.74
25	0	0	0	0	85.74	60.02
26	0	0	0	0	86.17	63.74
27	0	0	0	0	85.40	61.76
28	0	0	0	0	85.89	60.22

Table 5 show the results for the analysis of variance (ANOVA) for  $f_1$  and  $T_1$ . The results of the ANOVA in Table 5 show that the determination coefficients ( $R^2$ ) for  $f_1$  and  $T_1$  are 99.46% and 99.07%, respectively, so the two second-order models are significant. The results in Table 5 show that  $D$ ,  $W$ ,  $D_2$  and  $L$  are the significant parameters for  $f_1$ , and that  $D$ ,  $W$  and  $D_2$  are the important parameters for  $T_1$ .  $L$  has the greatest effect, followed by  $D$  and  $D_2$  in that order,

and  $W$  has the least effect for  $f_1$ . As the  $L$  decreases,  $f$  increases due to the extrusion effect between the tool and the metal material. However, considering the thickness limit of the cover of 3C smart electronic products, the  $L$  must be small enough. The values of  $D$ ,  $W$  and  $D_2$  have a significant effect on the  $f$  because there is a metal formed effect during tapping using a MFT (Warrington et al., 2005). The larger the  $D$ ,  $W$  and  $D_2$ , the larger is the  $f$ . The results in Table 5 also show that the first-order interaction factor  $DD_2$ ,  $WL$  and  $D_2L$  have a significant effect on  $f_1$ . Besides,  $D$  has the greatest effect, followed by  $W$  and  $D_2$  in that order, and  $L$  has the least effect for  $T$ .  $T$  increases with increasing  $D$ ,  $W$  and  $D_2$  due to the friction force and formed effect between the tool and the metal material. The  $D$ ,  $W$  and  $D_2$  have a significant effect to avoid excessive  $T$  during tapping using a MFT. The larger the  $D$ ,  $W$  and  $D_2$ , the larger is the  $T$ .  $L$  will affect tool life and tapping quality. Larger  $L$  will have smaller tapping torque (Landeta et al., 2015). However,  $L$  is still limited by the cover thickness of the 3C smart electronic products. The results in Table 5 also show that the first-order interaction factor  $DW$ ,  $DD_2$ ,  $DL$ ,  $WL$  and  $D_2L$  have a significant effect on  $T_1$ .

Table 5. ANOVA for  $f_1$  and  $T_1$

ANOVA	P VALUE (P<0.05)			
	$f_1$		$T_1$	
$R^2$	99.46%		99.07%	
F-TEST	171.99		98.89	
	T-value	P value	T-value	P value
INTERCEPT	398.28	0.000	91.58	0.000
$D$	20.05	0.000	25.76	0.000
$W$	7.14	0.000	20.47	0.000
$D_2$	-7.79	0.000	7.93	0.000
$L$	-31.14	0.000	-0.81	0.434
$D^2$	3.12	0.008	10.26	0.000
$W^2$	15.06	0.000	8.74	0.000
$D_2^2$	-20.93	0.000	5.61	0.000
$L^2$	-3.52	0.004	5.88	0.000
$DW$	-0.78	0.451	-4.70	0.000
$DD_2$	-3.53	0.004	3.97	0.002
$DL$	1.62	0.128	-2.31	0.038
$WD_2$	1.06	0.310	1.14	0.273
$WL$	15.13	0.000	-5.58	0.000
$D_2L$	3.84	0.002	-3.08	0.009

In order to understand the prediction results of the regression model of  $f_1$  and  $T_1$  for MFTs, this study uses 8 sets of corner point experiments to verify. Table 6 shows the  $f_1$  and  $T_1$  results of 8 sets of corner point experiments. Table 7 shows a comparison of the experimental values of and prediction data for the  $f_1$  and  $T_1$ . The respective errors (%) in  $f_1$  and  $T_1$  are less than 4.3% and 4.4%, so the two second-order models are satisfactory.

Table 6.  $f_1$  and  $T_1$  results of selected 8 sets of corner point experiments

No.	$D$	$W$	$D_2$	$L$	$f_1$ (%)	$T_1$ (N-mm)
1	1	-1	-1	-1	93.45	70.17
2	-1	1	-1	-1	78.21	79.14
3	-1	1	1	-1	78.79	81.46
4	1	1	1	-1	79.44	106.61
5	1	-1	-1	1	73.73	79.52
6	1	1	-1	1	81.58	82.23
7	-1	1	1	1	80.73	72.29
8	1	1	1	1	83.62	94.10

Table 7. Comparison of 8 sets experimental values and predicted values

No.	$f_1$ (%)			$T_1$ (N-mm)		
	Experiment	Prediction	Error (%)	Experiment	Prediction	Error (%)
1	93.45	90.34	3.44	70.17	73.34	-4.32
2	78.21	79.79	-1.98	79.14	78.96	0.23
3	78.79	77.72	1.38	81.46	83.89	-2.90
4	79.44	80.48	-1.29	106.61	105.99	0.58
5	73.73	75.12	-1.85	79.52	81.85	-2.85
6	81.58	83.42	-2.21	82.23	83.92	-2.01
7	80.73	77.45	4.23	72.29	75.39	-4.11
8	83.62	81.62	2.45	94.10	91.26	3.11

**Optimization analysis**

Based on the convenience of MFT manufacturers,  $f$  is widely used to evaluate the quality of internal thread tapping. Therefore, this study is to explore how to obtain the combination of the optimal tool quality parameter on  $T$  for SUS 316L stainless steel tapping under the  $f$  limitation conditions, and the upper and lower limits of the set quality parameters. Therefore, the mathematical model of the optimization constraint problem in this study can be expressed as follows:

$$\begin{cases} \text{Objective function: Min } T_{2s} \\ \text{Limitation condition: } f_{2s} - E(f_{2s}) \leq 0 \end{cases} \quad (5)$$

where  $T_{2s}$  is the optimal solution for the minimum tapping torque,  $f_{2s}$  is the optimal solution for the thread filling rate and  $E(f_{2s})$  is the expected value for  $f_{2s}$ , which is 85% (target). According to Eq. (5), the  $f_{2s}$  must be less than or equal to 85%. The coded variables for the optimal solution that is obtained using MINITAB software are shown in Table 8. The code value for  $D$  is -0.9742 (1.2353 mm). The smaller the  $D$ , the smaller is the friction force between the tool and the workpiece, so the smaller is the tapping torque and the greater is the thread filling rate. The code value of  $W$  is -0.9573 (0.9523 mm). Reducing the  $W$  reduces the friction force between the tool and the workpiece so the tool is not breakage by over-torque. The metal formed effect during tapping is also significant so the  $f$  increases (Warrington et al., 2005). The code value of  $D_2$  is

-0.9282 (0.9268 mm). However, this result is alike the  $W$ . As the code value of  $L$  is -0.9734 (0.2571 mm)  $T_1$  decreases but the value of  $f_1$  (T-value) increases faster as shown in Table 5.

Table 8. Optimal solution with the BBD

	$D$	$W$	$D_2$	$L$
Coded variable	-0.9742	-0.9573	-0.9282	-0.9734
(Real value)	(1.2353)	(0.9523)	(0.9268)	(0.2571)

In order to confirm the result of the prediction model, the optimal solution is experimentally tested. The error between the predicted and examination values for  $f_{2s}$  and  $T_{2s}$  are shown in Table 9. The results in Table 9 show that the examination results for the optimal solution are 84.21% and 48.54 N-mm for  $f_{2s}$  and  $T_{2s}$ , respectively. Compared to the predicted condition, the error results for the measurements for  $f_{2s}$  and  $T_{2s}$  are 0.94% and 3.58%, respectively. The prediction models with optimized quality parameters for  $f_{2s}$  and  $T_{2s}$  are proven to be efficient and industrially applicable.

Table 9. Comparison of the optimal solution on  $f_{2s}$  and  $T_{2s}$

Condition	$f_{2s}$ (%)	Error (%)	$T_{2s}$ (N-mm)	Error (%)
Prediction	85.00	-	50.34	-
Examination	84.21	0.94	48.54	3.58

**CONCLUSIONS**

MFT is one of the most critical tools in the process of internal thread less than 2 mm. The present paper aimed to obtain the optimum geometric dimensions of MFTs in SUS 316l stainless steel tapping. This study combines BBD and second-order RSM to discuss the quality characteristics of MFT for SUS 316L stainless steel tapping. Under the  $f$  limitation conditions and the upper and lower limits of the set quality parameters, the optimal tool quality parameter combination of MFT for SUS 316L stainless steel tapping torque is obtained. According to the experimental results of this study, the following conclusions can be drawn:

- (1) The quality characteristics ( $f$  and  $T$ ) of this study are based on second-order polynomials (including interaction terms) to establish two prediction models, and the prediction models are verified through 8 sets of corner point experiments to confirm the accuracy of the prediction models of quality characteristics in this study.
- (2) The four quality parameters ( $D$ ,  $W$ ,  $D_2$  and  $L$ ) have significant influence on  $f$ , especially,  $L$  has the most significant influence. When  $D$  and  $W$  are larger,  $f$  is higher; and  $L$  and  $D_2$  are larger,  $f$  is lower.

(3) The effects of  $D$ ,  $W$  and  $D_2$  on  $T$  are more significant. Among them,  $D$  has the most significant influence. When  $D$ ,  $W$  and  $D_2$  are larger,  $T$  is larger.

(4) The parameter encoding levels of the optimal MFT geometry obtained by BBD are  $D=-0.9742$  (1.2353 mm),  $W=-0.9573$  (0.9523 mm),  $D_2=-0.9282$  (0.9268 mm) and  $L=-0.9734$  (0.2571 mm). The examination results for the optimal solution are 84.21% and 48.54 N-mm for  $f_{2s}$  and  $T_{2s}$ , respectively. The error results for the measurements for  $f_{2s}$  and  $T_{2s}$  are 0.94% and 3.58%, respectively.

## ACKNOWLEDGMENT

Financial support for this work was provided by the National Science Council Taiwan, R.O.C, under the contract MOST 108-2221-E-262-002-MY2.

## REFERENCES

- Agapiou, J.S., "Evaluation of the Effect of High Speed Machining on Tapping." *ASME J. Eng. Ind.*, Vol. 116, pp. 457-462 (1994).
- Carvalho, A.O., Brandão, L.C., Panzera, T.H., and Lauro, C.H., "Analysis of Form Threads Using Fluteless Taps in Cast Magnesium Alloy (AM60)." *J. Mater. Process. Technol.*, Vol. 212, pp. 1753-1760 (2012).
- Chowdhary, S., Ozdoganlar, O.B., Kapoor, S., and DeVor, R., "Modeling and Analysis of Internal Thread Forming." *Trans. NAMRC/SME*, Vol. 30, pp. 329-336 (2002).
- Fromentin, G., Poulachon, G., and Moisan, A., "An Experimental and Analytical Method for Investigating Plastic Flow in Form Tapping." *Int. J. Form Process.*, Vol. 9, pp. 457-472 (2006).
- Hou, H.L., Zhang, G.P., Xin, C., and Zhao, Y.Q., "Numerical Simulation and Process Optimization of Internal Thread Cold Extrusion Process." *Mater.*, Vol. 13, No. 18, pp. 6-13 (2020).
- ISO 68-1: General Purpose Screw Threads- Basic Profile- Part 1: Metric Screw Threads (1998).
- Landeta, J.F., Valdivielso, A.F., de Lacalle, L.N.L., Giro, F., and Pérez, J.M., "Wear of Form Taps in Threading of Steel Cold Forged Parts." *ASME J. Manuf. Sci. Eng.*, Vol. 137, 031002\_1-031002\_11 (2015).
- Mathurin, F., Guillot, J., Stéphan, P., and Daidié, A., "3D Finite Element Modeling of An Assembly Process with Thread Forming Screw." *J. Manuf. Sci. Eng.*, Vol. 131, pp. 151-158 (2009).
- Oliveira, J., Filho, S., and Brandão, L., "Investigation of the Influence of Coating and the Tapered Entry in the Internal Forming Tapping

- Process." *Int. J. Adv. Manuf. Technol.*, Vol. 101, pp. 1051-1063 (2019).
- Sakurai, K., Sawai, T., and Adachi, K., "Performance of TiN Coated Flute-less Tap on 15% SiC Particle Reinforced 2618 Aluminum Alloy Tapping." *J. Japan Inst. Light Met.*, Vol. 56, pp. 301-306 (2006).
- Stéphan, P., Mathurin, F., and Guillot, J., "Analytical Study of Maximal Tapping Torque during Forming Screw Process." *J. Mater. Process. Technol.*, Vol. 211, pp. 212-221 (2010).
- Tállai, P., Csuka, S., and Sipos, S., "Thread Forming Tools with Optimised Coatings." *Acta Polytech. Hung.*, Vol. 12, pp. 55-66 (2015).
- Warrington, C., Kapoor, S.G., and DeVor, R.E., "Experimental Investigation of Thread Formation in Form Tapping." *ASME J. Manuf. Sci. Eng.*, Vol. 127, pp. 829-836 (2005).

## 微成形絲攻於 SUS 316L 不銹鋼攻牙之最佳幾何尺寸研究

鄧翔明

國立臺灣師範大學工業教育學系

陳建中

敏實科技大學智慧汽車與能源系

許永翰

國立中央大學機械工程系

吳明昌 曹中丞

龍華科技大學機械工程系

許靈生

合鑽機械股份有限公司

## 摘要

本研究旨在根據微成形絲攻(Micro-Forming Tap, MFT)的幾何參數(外徑( $D$ )、刀具寬度( $W$ )、齒根直徑( $D_2$ )和無效齒長度( $L$ ))開發一種新的攻牙刀具設計,以克服針對 SUS 316L 不銹鋼攻牙時使用傳統絲攻的刀具破損(攻牙扭力)、加工效率低、排屑等缺陷的問題。同時,透過 Box-Behnken 設計和回歸分析,建立品質特性的二階響應面模型,並確定 M1.2 的最小絲攻扭矩( $T$ )和飽牙率( $f$ )的最佳刀具幾何參數。最後實驗結果顯示,本研究得到的  $T$  和  $f$  預測模型以及 MFT 的最佳幾何參數是相當準確和一致的。